

# **Supplemental Material**

- Tables and Captions  
(Tables I-IV)
- Figures (Figs. I-VII)
- Material and Methods

### Online Table I. Postmortem Analysis

|                   | Ctrl        | HF              | CHF                  |
|-------------------|-------------|-----------------|----------------------|
| No. of animals    | 12          | 10              | 5                    |
| BW (g)            | 32.2 ± 1.1  | 31.7 ± 1.0      | 26.0 ± 0.7 ** ##     |
| HW (mg)           | 155 ± 2.3   | 203 ± 9.7 ***   | 305.4 ± 6.9 *** ###  |
| LVW(mg)           | 120.9 ± 2.0 | 162.0 ± 9.7 *** | 232.6 ± 6.2 *** ###  |
| HW/BW (mg/g)      | 4.8 ± 0.1   | 6.5 ± 0.4 ***   | 11.3 ± 0.2 *** ###   |
| LVW/BW (mg/g)     | 3.80 ± 0.12 | 5.17 ± 0.36 *** | 8.59 ± 0.30 *** ###  |
| LW/BW (mg/g)      | 4.25 ± 0.15 | 5.11 ± 0.27 **  | 18.96 ± 0.43 *** ### |
| Tibia Length (mm) | 18.0 ± 0.1  | 17.9 ± 0.1      | 17.7 ± 0.2           |

Body Weight (BW), Heart Weight (HW), Left Ventricle weight (LVW), Lung weight (LW).  
 \*P<0.05, \*\*P<0.01, \*\*\*P<0.001 vs sham-operated controls. #P<0.05, ##P<0.01,  
 ###P<0.001 vs Heart Failure TAC mice.

## Online Table II. Echocardiography

|  | Ctrl         | HF             | CHF              |
|--|--------------|----------------|------------------|
| No. of animals                             | 13           | 10             | 7                |
| Heart Rate (BPM)                           | 503 ± 20     | 486 ± 15       | 502 ± 21         |
| <b>M-Mode Protocol</b>                     |              |                |                  |
| LV Vol;d (ml)                              | 58 ± 2.7     | 83 ± 7.4 **    | 97 ± 3.9 ***     |
| LV Vol;s (ml)                              | 26 ± 2.4     | 48 ± 6.7 **    | 56 ± 4.5 ***     |
| LVID;d (mm)                                | 3.7 ± 0.1    | 4.3 ± 0.2 **   | 4.6 ± 0.1 ***    |
| LVID;s (mm)                                | 2.6 ± 0.1    | 3.4 ± 0.2 **   | 3.6 ± 0.1 ***    |
| IVS;d (mm)                                 | 1.0 ± 0.04   | 1.1 ± 0.03     | 1.2 ± 0.05 **#   |
| IVS;s (mm)                                 | 1.2 ± 0.04   | 1.3 ± 0.04     | 1.5 ± 0.05 **##  |
| LVPW;d (mm)                                | 1.0 ± 0.04   | 1.1 ± 0.04     | 1.2 ± 0.04 **#   |
| LVPW;s (mm)                                | 1.7 ± 0.04   | 1.3 ± 0.04     | 1.5 ± 0.05 **##  |
| %EF (%)                                    | 57 ± 3       | 44 ± 3 **      | 43 ± 3**         |
| % FS (%)                                   | 29 ± 2       | 23 ± 2 *       | 21 ± 2 **        |
| LV Mass (mg)                               | 117 ± 6.6    | 169 ± 14.1 **  | 217 ± 9.6 ***#   |
| <b>Pulse-Wave Doppler analysis</b>         |              |                |                  |
| Pressure gradient (PG, mm Hg) <sup>a</sup> | -----        | 56.3 ± 4.6 *** | 85.6 ± 4.6 ***## |
| MV E (m/s)                                 | 0.69 ± 0.03  | 0.76 ± 0.05    | 0.87 ± 0.05 **   |
| MV A (m/s)                                 | 0.42 ± 0.02  | 0.33 ± 0.03 *  | 0.21 ± 0.03 ***# |
| MV E / A                                   | 1.58 ± 0.05  | 2.66 ± 0.51 *  | 4.86 ± 0.90 ***# |
| DT (msec)                                  | 21.0 +/- 0.8 | 21.8 +/- 0.6   | 19.6 +/- 0.9 #   |

LV diastolic volume (LV Vol;d), LV systolic volume (LV Vol;s), LV internal diastolic diameter (LVID; d), LV internal systolic diameter (LVID;s), Inter ventricular septum, diastolic (IVS;d), Inter ventricular septum, systolic (IVS;s), LV posterior wall, diastolic (LVPW;d), LV posterior wall, systolic (LVPW;s), LV Ejection fraction (EF), LV Fractional shortening (FS), Mitral valve E velocity (MV E), Mitral valve A velocity (MV A), and the deceleration time of the E wave (DT) \*P<0.05, \*\*P<0.01, \*\*\*P<0.001 vs sham-operated controls. #P<0.05, ##P<0.01 vs Heart Failure TAC mice. <sup>a</sup>Calculated from the peak blood velocity (V<sub>max</sub>) (m/s) (PG=4 V<sub>max</sub><sup>2</sup>) measured by Doppler across the aortic constriction.

### Online Table III Protein Analysis

|                     | Ctrl        | HF            | CHF             |
|---------------------|-------------|---------------|-----------------|
| No. of animals      | 5           | 5             | 6               |
| MHC (OD/mg)         | 33.9 ± 4.2  | 35.7 ± 4.1    | 33.0 ± 4.0      |
| Total Titin (OD/mg) | 8.93 ± 1.00 | 7.14 ± 1.54   | 8.13 ± 1.75     |
| Total Titin/MHC     | 0.24 ± 0.01 | 0.26 ± 0.04   | 0.28 ± 0.03     |
| N2BA/N2B            | 0.22 ± 0.02 | 0.29 ± 0.03 * | 0.36 ± 0.02 *** |
| T2/Total Titin      | 0.13 ± 0.02 | 0.09 ± 0.01   | 0.10 ± 0.02     |

\*P<0.05, \*\*\*P<0.001 vs sham-operated controls.

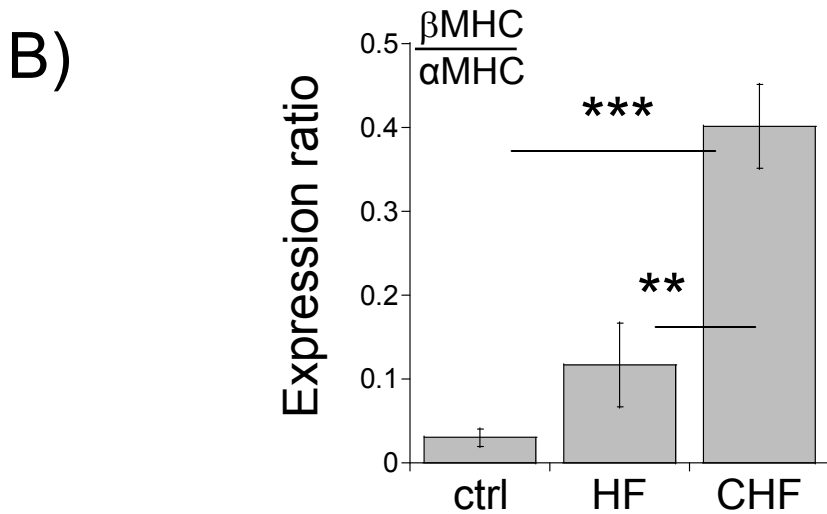
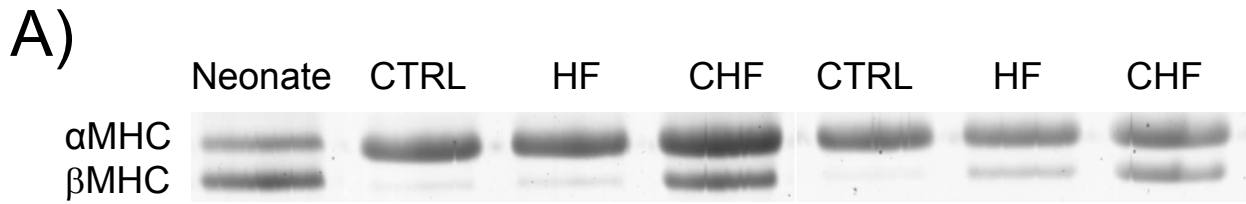
## On line Table IV. Transcript analysis.

Titin exon microarray analysis comparing CHF with control LV tissues. All differentially expressed exons are shown. 35 exons are upregulated in CHF and 3 down regulated. All differential exons are in the Z-disk or titin's extensible I-band.

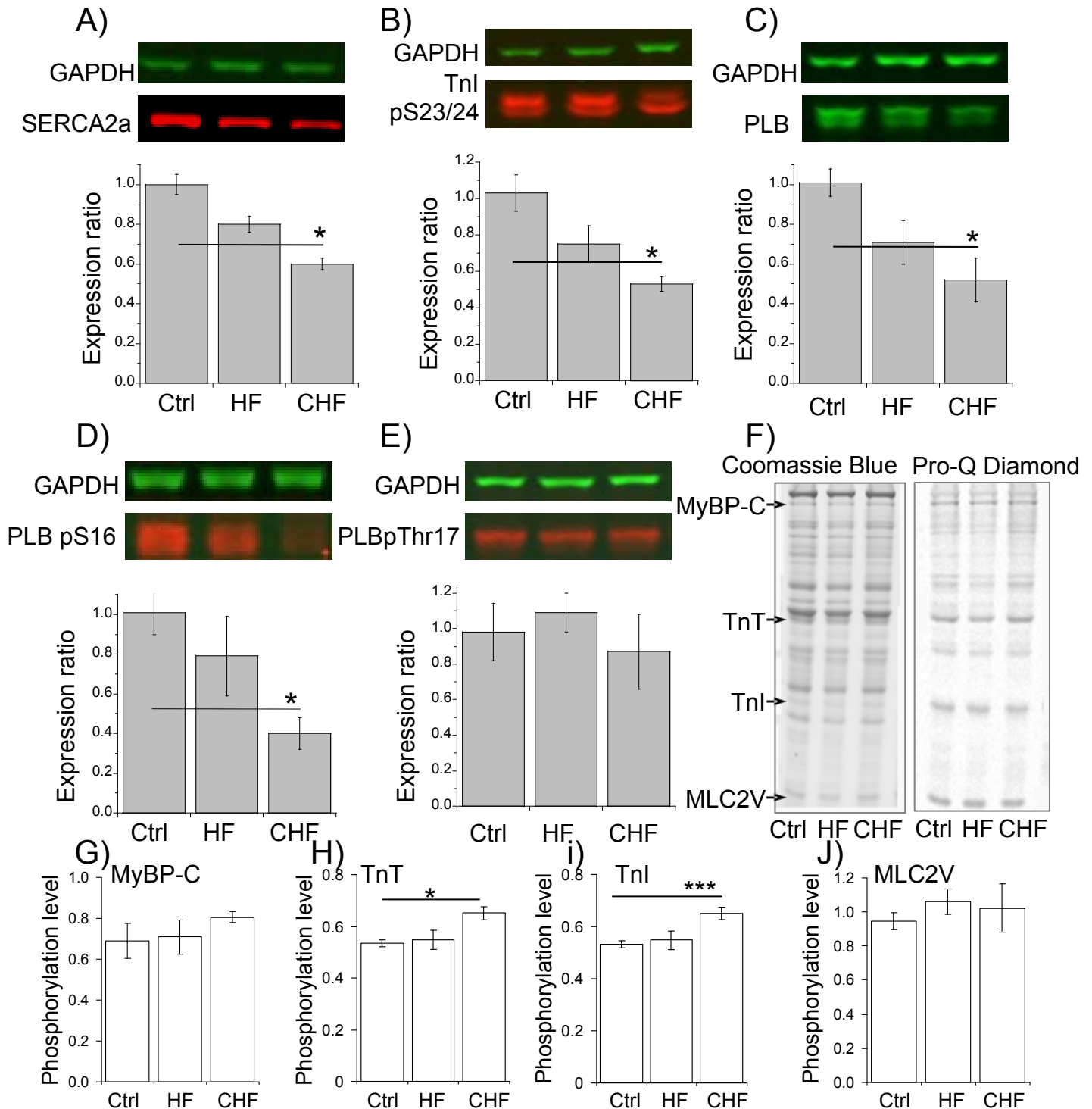
| Upregulated exons |                   | Upregulated exons |                   | Downregulated |                    |
|-------------------|-------------------|-------------------|-------------------|---------------|--------------------|
| MTE1              | 2.69 +/- 0.10 **  | MTE162            | 1.58 +/- 0.11 *   | MTE115        | -1.68 +/- 0.05 *** |
| MTE2              | 2.52 +/- 0.10 **  | MTE163            | 1.61 +/- 0.06 **  | MTE117        | -1.68 +/- 0.04 *** |
| MTE3              | 2.53 +/- 0.04 *** | MTE173            | 2.02 +/- 0.11 **  | MTE242        | -1.53 +/- 0.06 **  |
| MTE4              | 1.57 +/- 0.09 *   | MTE189            | 1.82 +/- 0.10 **  |               |                    |
| MTE5              | 2.22 +/- 0.07 **  | MTE190            | 1.98 +/- 0.05 *** |               |                    |
| MTE6              | 2.35 +/- 0.06 *** | MTE191            | 1.77 +/- 0.08 **  |               |                    |
| MTE15             | 1.68 +/- 0.05 **  | MTE192            | 1.83 +/- 0.08 **  |               |                    |
| MTE16             | 1.78 +/- 0.12 *   | MTE194            | 1.89 +/- 0.12 **  |               |                    |
| MTE54             | 1.81 +/- 0.09 **  | MTE196            | 2.25 +/- 0.05 *** |               |                    |
| MTE66             | 1.56 +/- 0.09 *   | MTE197            | 2.06 +/- 0.07 **  |               |                    |
| MTE72             | 2.24 +/- 0.08 **  | MTE198            | 1.62 +/- 0.11 *   |               |                    |
| MTE81             | 1.69 +/- 0.10 *   | MTE200            | 1.94 +/- 0.07 **  |               |                    |
| MTE82             | 1.76 +/- 0.04 **  | MTE202            | 1.69 +/- 0.06 **  |               |                    |
| MTE85             | 1.54 +/- 0.08 *   | MTE208            | 1.82 +/- 0.11 *   |               |                    |
| MTE86             | 1.80 +/- 0.07 **  | MTE214            | 1.51 +/- 0.04 **  |               |                    |
| MTE87             | 1.85 +/- 0.05 **  | MTE215            | 1.52 +/- 0.08 *   |               |                    |
| MTE130            | 2.18 +/- 0.06 **  | MTE216            | 1.54 +/- 0.07 **  |               |                    |
| MTE137.5          | 1.58 +/- 0.10 *   |                   |                   |               |                    |

Blue: Z-disk exons;  
 Extensible I-band region:  
 --Red: Ig exons;  
 --Yellow: PEVK exons.

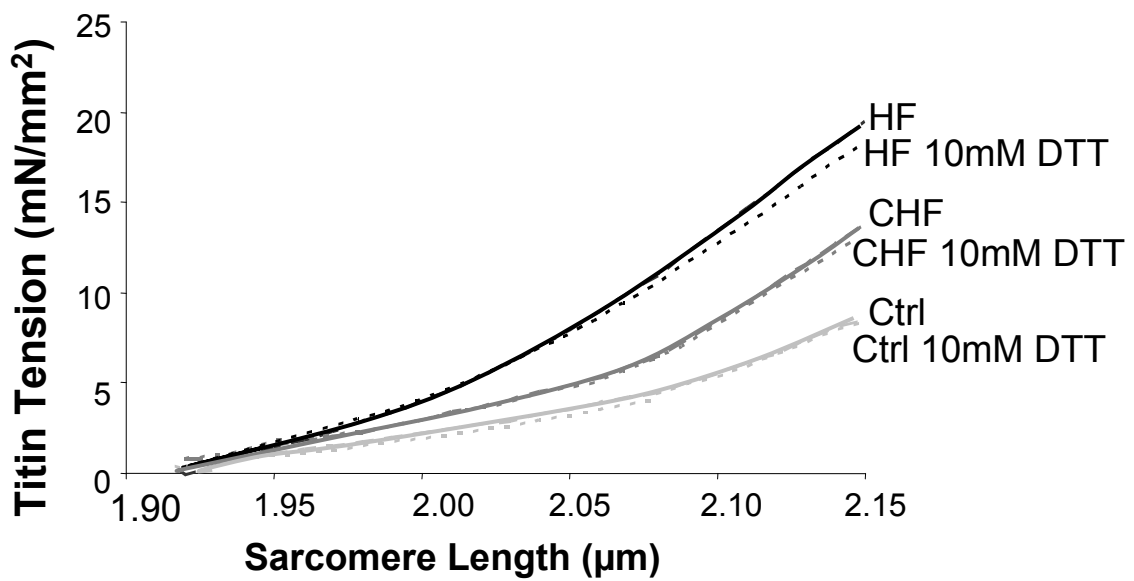
\*P<0.05, \*\*P<0.01, \*\*\*P<0.001 vs sham-operated controls.



**On line Figure I. Myosin Heavy Chain (MHC) expression in LV of control (Ctrl), heart failure (HF), and congestive heart failure (CHF) mice.** A) Representative examples of  $\alpha$ MHC and  $\beta$ MHC isoform expression in representative samples. A 1-day old neonatal sample that expresses both  $\alpha$ MHC and  $\beta$ MHC is shown for reference. Following TAC-induced heart failure, there is a clear shift from the predominant  $\alpha$ MHC isoform towards the  $\beta$ MHC isoform, with the most pronounced shift occurring in the CHF hearts. Bar graphs in B show expression ratio of 6 Ctrl, 6 HF, and 6 CHF samples (mean  $\pm$  SEM).

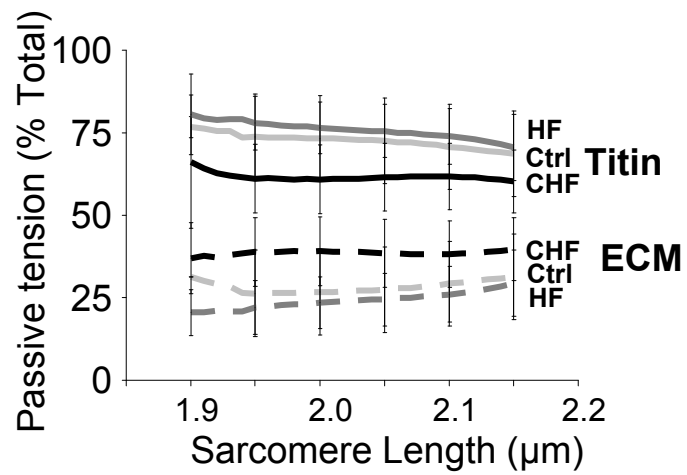


**Online Figure II. Protein expression and phosphorylation levels in LV of Ctrl, HF, and CHF mice.** A-E: WB-based expression of A) SERCA2a, B) phospholamban (PLB), C) pS16 of PLB, D) pThr17 of PLB, and E) pS23/24 of cTnI. GAPDH is used as a loading control. Expression of SERCA2a, PLB, PLBpS16 and TnIpS23/24 is significantly reduced in the CHF mice whereas PLBpThr17 is unaltered. Bar graphs are mean  $\pm$  SEM expression levels normalized to GAPDH (n= 6 per group). Levels are relative to those in the control mice. D-H) Pro-Q Diamond staining to reveal total protein phosphorylation of cMyBP-C, TnT, TnI and MLC2V. F: Representative samples. G-J): Phosphorylation levels of cMyBP-C (G), TnT (H), TnI (i) and MLC2V (J). Pro-Q Diamond staining normalized to Coomassie Blue staining. Because Pro-Q Diamond reports total phosphorylation, disparate results between Pro-Q diamond staining and specific phosphorylation sites probed with phospho-antibodies (compare B and G) can be expected. (4 mice per group.)

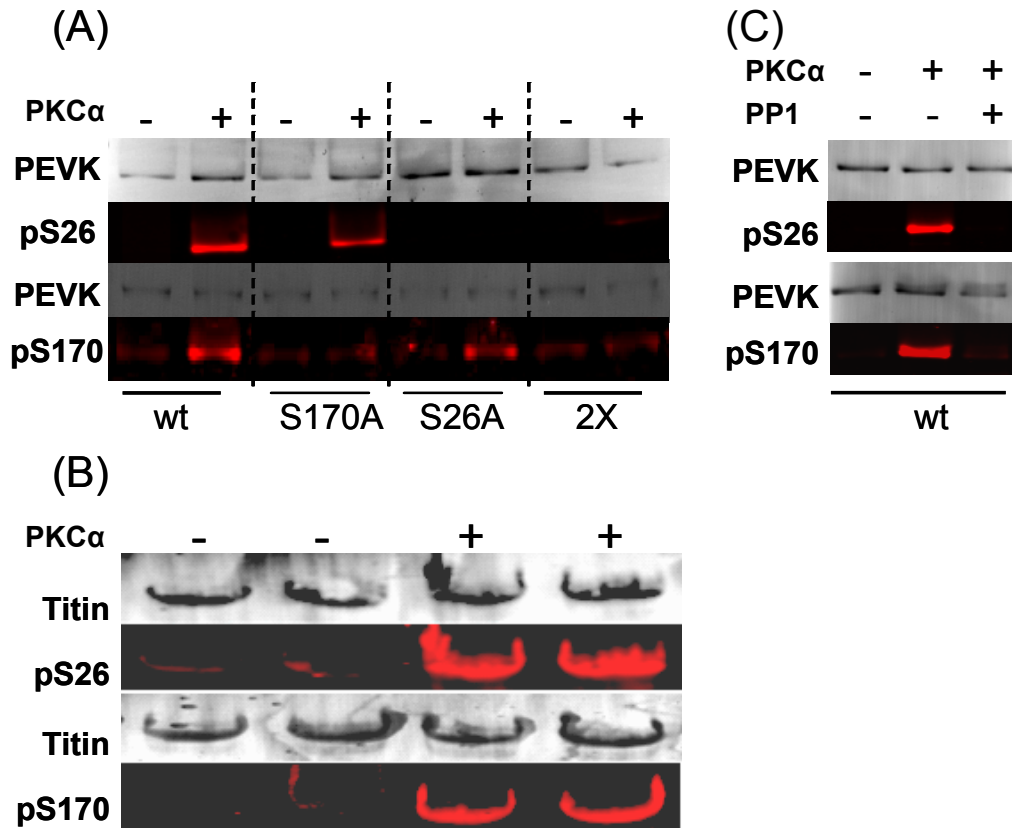


**Online Figure III. Effect of increased DTT concentration on myocardial passive stiffness.** To evaluate the effect of potential oxidizing conditions on myocardial stiffness we incubated the LV samples in high concentrations of the reducing agent, DTT (10mM) and stretched to SL 2.15. Passive stiffness was not altered following incubation with 10mM DTT.

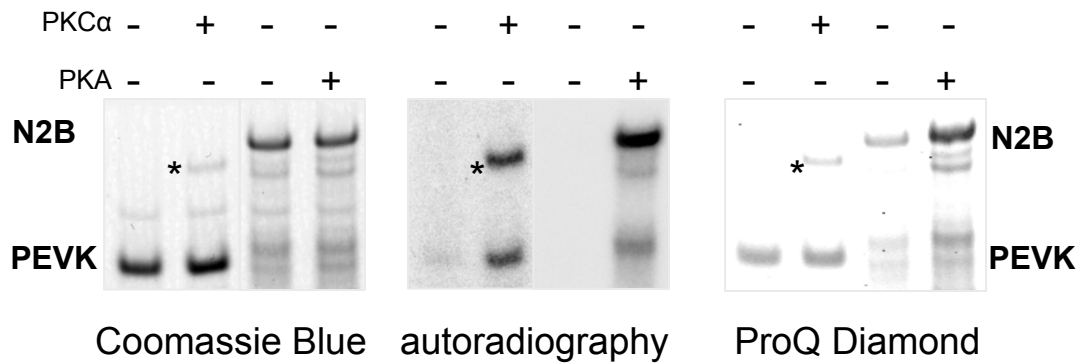




**On line Figure IV. Sources of passive stiffness.** Comparison of the relative contribution of titin and collagen to the overall passive tension in Ctrl, HF, and CHF groups. Results indicate that titin is the major contributor to passive tension in all three groups.



**Online Figure V. Validation of pS26 and pS170 antibodies against PKC $\alpha$ -induced phosphorylation of titin and effect of protein phosphatase 1 (PP1).** (A) Validation using recombinant PEVK protein without (-) or with (+) PKC $\alpha$  phosphorylation; both pS26 and pS170 recognize phosphorylation following PKC $\alpha$  incubation in wt PEVK. Each antibody is specific, as mutation of the target serine to alanine abolishes antibody binding (S170A and S26A). In the double mutation (2X), where both S26 and S170 have been mutated to alanine, neither antibody has any specific binding. (B) We also tested the antibodies on mouse LV without (-) or with (+) PKC $\alpha$ . Both antibodies strongly label phosphorylated titin. (C) Effect of PP1 on PKC $\alpha$  phosphorylated WT PEVK (top pS26, bottom pS170). PKC $\alpha$  phosphorylates both S26 and S170 and PP1 dephosphorylates these sites.



\* PKC $\alpha$

**On line Figure VI. ProQ-diamond stain does not detect PEVK phosphorylation.** Phosphorylation of recombinant N2B protein with PKA can be easily detected with both autoradiography and ProQ-diamond whereas PKC $\alpha$  phosphorylation of PEVK protein is only detected with autoradiography and not ProQ-diamond. (\* PKC $\alpha$  which autophosphorylates)

|               | 11867    | 11878 (S26) | 12014          | 12022 (S170) |       |                  |
|---------------|----------|-------------|----------------|--------------|-------|------------------|
| Human         | PKEEVVLK | S           | VLRKRPEEEEEPKV | KLRPG        | S     | GGGEKPPDEAPFTYQL |
| Rhesus monkey | PKEEVVLK | S           | VLRKRPEEEEEPKV | KLRPG        | S     | GGGEKPPDEAPFTYQL |
| Chimpanzee    | PKEEVVLK | S           | VLRKRPEEEEEPKV | KLRPG        | S     | GGGEKPPDEAPFTYQL |
| Cow           | PKEEVVLK | S           | VLRKKPEEEEEPKV | KLRPG        | S     | GGGEKPPDEAPFTYQL |
| Horse         | PKEEVVLK | S           | VLRKKPEEEEEPKV | KLRPG        | S     | GGGEKPPDEAPFTYQL |
| Rabbit        | PKEEVVLK | S           | VLRKRPEEEEEPKV | KLRPG        | S     | GGGEKPPDEAPFTYQL |
| Dog           | PKEEVVLK | S           | VLRKRPEEEEEPKV | KLRPG        | S     | GGGEKPPDEAPFTYQL |
| Pig           | PKEEVVLK | S           | VLRKRPEEEEEPKV | KLRPG        | S     | GGGEKPPDEAPFTYQL |
| Mouse         | PKEEVVLK | S           | VLRKKPEEEEEPKV | KLRPG        | S     | GGGEKPPDEAPFTYQL |
| Rat           | PKEEVVLK | S           | VLRKRPEEEEEPKV | KLRPG        | S     | GGGEKPPDEAPFTYQL |
|               | *****    | *****       | *****          | *****        | ***** | *****            |

**On line Figure VII. PEVK sequence alignment around S26 (left) and S170 (right).** More basic residues are found within a 3 residue span from the S26 site than the S170 site. See text for details.

## Supplemental Materials and Methods

**Transverse Aortic Constriction.** For Transverse Aortic Constriction (TAC) surgeries, a mixture of Avertin (2,2,2 tribromoethanol, Aldrich T4,840.2) (0.5mg/kg), Acepromazin (1mg/kg), and Ketamine (1mg/kg) was injected intraperitoneally in 60 day old male C57BL/6J mice. This mixture provides an adequate depth of anesthesia for 50–60 min which is long enough to finish the surgery. The aortic banding procedure was performed similar to that previously described<sup>1-2</sup> with minor adaptations. Briefly, the chest cavity was opened and the ascending portion of the aorta was bluntly dissected from the pulmonary trunk. A curved forceps was then placed under the transverse aorta, 7-0 silk was grasped by the forceps and moved underneath the aorta, and a loose double knot was made. A 27-gauge needle with OD 0.42 mm was delivered through the loose double knot and placed directly above and parallel to the aorta. The loop was then tied around the aorta and needle and secured with the second knot (this was done very quickly, to minimize ischemia). The needle was immediately removed to provide a lumen with a stenotic aorta. Following the surgery, all layers of muscle and skin were closed with 6-0 continuous absorbable and nylon sutures, respectively, and the wound was treated with Betadine. Immediately after the operation, 0.5 ml of 37°C saline was given intraperitoneally, and a dose of analgesic (buprenorphine, 0.1 mg/kg) was also given subcutaneously; further analgesic was administered every 8 h for the next 48 h. For the sham operation (control) the mice underwent the identical procedure, except placing of the ligature. The surgical survival rate following TAC was ~90% and mortality rate within the first month following TAC was low (<5%). Successful surgical ligation of the transverse aorta, determined by a Doppler flow velocity measurement (see below), indicated a large pressure gradient following constriction (see online Table II). TAC and sham animal heart function were evaluated 8 weeks after surgery, using echocardiography. Following this, animals were sacrificed, weighed (BW) and total heart weights (HW), LV weights (LVW), lung weights (LW), and tibia length were determined. Hearts were immediately dissected (see Animals and Tissue collection below) (removal of papillaries for muscle mechanics and splitting the LV into bilateral halves). Bilateral halves were either frozen or stored in RNA $\text{later}$ . Animals were divided into 2 groups based on both LVW/BW (HF 4.25mg/g-6.75mg/g; CHF>6.75mg/g) and LW/BW (HF

4.5mg/g-12mg/g; CHF>12mg/g) (see Figure 1), since LV mass and pleural edema both correlate with degree of heart failure development <sup>3</sup>.

**Echocardiography.** Echocardiography was performed similar to as described previously<sup>4</sup>. Briefly, anesthesia induction was performed with 2% ISOFLOR (Abott, Abott Park, IL) in a Univentor 400 anesthesia chamber. Following anesthesia, the mouse was placed in dorsal recumbence on a heated, tilt platform for echocardiography. Body temperature was maintained at 37°C, and anesthesia was continued with 0.5-1.5% ISOFLOR. Transthoracic ECHO images were obtained with a Vevo 700 High Resolution Imaging System (Visual-Sonics, Toronto, Canada), using the model 707B scan head designed for murine cardiac imaging. A standoff was created for the ultrasound transducer using conductivity gel. Care was taken to avoid animal contact and excessive pressure which can induce bradycardia. Imaging was performed at a depth setting of 1 cm. Images were collected and stored as a digital cine loop for off-line calculations. Standard imaging planes, M-mode, Doppler, and functional calculations were obtained according to American Society of Echocardiography guidelines. The parasternal long-axis four-chamber view of the left ventricle (LV) was used to guide calculations of percentage fractional shortening, percentage ejection fraction, and ventricular dimensions and volumes. A right supra-clavicular view was used to measure cardiac output, calculated with aortic diameter and aortic flow velocity time index. In addition, the left atrial dimension was measured in the long-axis view directly below the aortic valve leaflets. Passive LV filling peak velocity, E (cm/s), and atrial contraction flow peak velocity, A (cm/s), were acquired from the images of mitral valve Doppler flow from a four chamber view. The E-A velocity time index (E-AVTI) was the computed velocity time integral of both E and A wave forms. The E/E-A VTI ratio is an index of diastolic function independent of preload. The Ea and Aa were the tissue peak velocity of the LV adjacent to the mitral valve annulus. For pulsed-wave Doppler recording, a sample size of 0.3 mm was used. A sweep speed of 100 mm/s was used for M-mode and Doppler studies.

**Animals and tissue collection.** Mouse left ventricular (LV) and papillary muscles were collected from male BL6 mice 8 weeks following TAC surgery (see below). Mice were anesthetized with isoflurane (Abbott Laboratories, Chicago, IL) and sacrificed by cervical dislocation. The hearts were rapidly excised and the muscles dissected (collection of papillaries and LV) in oxygenated HEPES pH 7.4 (in mM: NaCl, 133.5; KCl, 5; NaH<sub>2</sub>PO<sub>4</sub>,

1.2; MgSO<sub>4</sub>, 1.2; HEPES, 10) and weighed (Online Table 1). Dissected LV muscles were then divided into two pieces and: 1) snap frozen in liquid nitrogen, or 2) stored in RNAlater. Papillary muscles were skinned in relaxing solution pH 7.0 (RX) (in mM: BES 40, EGTA 10, MgCl<sub>2</sub> 6.56, Na<sub>2</sub>ATP 5.88, DTT 1, K-propionate 46.35, creatine phosphate 15) (chemicals from Sigma-Aldrich, MO, USA) with 1% Triton-X-100 (Pierce, IL, USA) overnight at ~3°C, then washed thoroughly with relaxing solution and stored for one month or less at -20°C in relaxing solution containing 50% (v/v) glycerol. To prevent protein degradation, all solutions contained protease inhibitors (phenylmethylsulfonyl fluoride (PMSF), 0.5 mM; Leupeptin, 0.04 mM; E64, 0.01mM). All animal experiments were approved by the University of Arizona Institutional Animal Care and Use Committee and followed the U.S. National Institutes of Health “Using Animals in Intramural Research” guidelines for animal use.

**Gel Electrophoresis.** For titin protein analysis, SDS–agarose electrophoresis was performed as previously described<sup>5</sup>. Briefly, muscle samples were solubilized in a urea and glycerol buffer and analyzed by vertical SDS–agarose electrophoresis. The 1% agarose gels were run at 15 mA per gel for 3 h and 20 min. The gels were stained with Coomassie brilliant blue (CBB), and subsequently scanned and analyzed using One-D scan EX (Scanalytics Inc., Rockville, MD, USA) software. The integrated optical density of titin and MHC was determined as a function of the volume of solubilized protein sample that was loaded (a range of volumes was loaded on each gel). The slope of the linear range of the relationship between integrated optical density and loaded volume was obtained for each protein.

**Western Blots ((WBs).** For titin Western blotting (WB) LV samples were run on 1% agarose gels, and transferred to PVDF membrane (Millipore, Immobilon®-FL Cat. No. IPFL00010) using a semi-dry transfer unit (Bio-Rad, Hercules, CA). The blots were stained with Ponceau S solution (SIGMA P7170) to visualize total transferred protein. The blots were then probed with rabbit polyclonal antibodies against titin’s pS26 (GenScript, 1:1000) and pS170 (Genscript, 1:250) against recombinant PEVK. On skinned fibers the antibodies were used against titin’s pS26 (GL Biochem, Shanghai, 1:1000) and pS170 (Genscript, 1:250). We also studied phosphorylation levels of S26 and S170 of skinned fibers that has been treated by PP1 (0.5 U/μl; for details, see Passive tension Measurement section, below) for 2 hours followed by WB analysis with

antibodies against pS26 and pS170. To normalize for loading differences, phosphorylated titin labeling was normalized to total protein, determined from the Ponceau S-stained membrane and analyzed with One-D scan EX. Secondary antibodies conjugated with fluorescent dyes with infrared excitation spectra were used for detection. One-color IR western blots were scanned (Odyssey Infrared Imaging System, Li-Cor Biosciences, NE, USA) and the images analyzed. We also performed a WB analysis of SERCA2A, PLB, pS23/24 cTnI, PLBpS16, and PLBpTrh17 with antibodies purchased from Badrilla LTD (Leeds, UK; catalog #A010-20), Badrilla LTD (Leeds, UK; catalog #A010-14), Cell Signaling Technology (Ma, USA, catalog # 4004S), Badrilla LTD (Leeds, UK; catalog #A010-12), Badrilla LTD (Leeds, UK; catalog #A010-13). Blots were dual labeled with an anti-GAPDH antibody (used as a loading control) that was from Abcam (Cambridge USA, ab8245).

### **Phosphorylation Assays**

*Detection of protein phosphorylation by protein labeling ( $^{32}P$ ) and phosphoprotein stain (Pro-Q diamond).* BL/6 mouse LV fibers were skinned in skinning solution pH 7.0 (in mM: 20 BES, 10 EGTA, 6.56 MgCl<sub>2</sub>, 5.88 Na<sub>2</sub>ATP, 1 DTT, 46.35 K-propionate, 15 creatine phosphate), and 1% (w/v) Triton X-100 (at 20°C). Subsequently, the skinned fibers were washed in relaxing solution (skinning solution without Triton X-100), and stored in relaxing solution containing 50% (v/v) glycerol at -20°C. Skinned fibers 2 mm in length, 0.5 mm in diameter were dissected. Two sets of skinned fibers were incubated with 1 U/μl of protein kinase A (PKA) catalytic subunit from bovine heart (Sigma) in relaxing solution or 0.066 U/μl of protein kinase C alpha (PKCα) (Enzo) in activating solution pH 7.0 (in mM: BES 16, CaCO<sub>3</sub>-EGTA 4, MgCl<sub>2</sub> 2.5, Na<sub>2</sub>ATP 2.4, DTT 0.85, K-propionate 18.1, creatine phosphate 6, NaCl 30, glycerol 5%), lipid activator (PS 0.2 mg/ml, DAG 0.02 mg/ml, triton X-100 0.6%), and 10 mM NaF, 2 mM Na<sub>3</sub>VO<sub>4</sub>). To one set 20 μCi of [ $\gamma$ - $^{32}P$ ]ATP stock solution, specific activity 3,000 Ci/mmol (PerkinElmer, USA) were added and the samples incubated 4h at RT. The reaction was stopped by adding solubilization buffer (6M urea, 2 M thiourea, 2.3% SDS, 58 mM DTT, 0.02% bromophenol blue, and 38.5 Tris HCl pH 6.8). The solubilized samples were electrophoresed on a 2 to 7% gradient SDS-PAGE and the gels were Coomassie blue stained, dried, and exposed to X-ray film. The dried gels and the autoradiography were scanned using Epson Expression 800 scanner. The images were analyzed with One-Dscan software (Scanalytics Inc) to obtain the integrated optical density. The titin



integrated OD of the autoradiograph was normalized to that of the Coomassie blue-stained gel, to normalize for protein loading. The other set of fibers was incubated as above but without radiochemical. The proteins were separated as above and the gel was stained with Pro-Q diamond to visualize proteins phosphorylated. The gel was fixed in 50% methanol 10% acetic acid, stained with Pro-Q diamond (Invitrogen), destained with 20% ACN 50 mM sodium acetate pH 4, and scanned with Typhoon 9400 (Amersham Biosciences) (excitation source 532 nm laser, emission filter 560 nm longpass). Then the gel was Coomassie blue stained to visualize total proteins and scanned as above. The Pro-Q diamond stain proteins were normalized to that of the Coomassie blue-stained gel to normalize for protein loading.

*Detection of recombinant protein phosphorylation by protein labeling ( $^{32}\text{P}$ ) phosphoprotein stain (Pro-Q diamond), and WB.* Two sets of purified recombinant titin fragments, N2B and PEVK, were incubated with 1 U/ $\mu\text{l}$  of PKA in relaxing solution or with 0.066 U/ $\mu\text{l}$  of PKC $\alpha$  in activating solution (described above). To one set 20  $\mu\text{Ci}$  of [ $\gamma$ - $^{32}\text{P}$ ]ATP was added and incubated for 4h at RT. Then the proteins were denatured with SDS-PAGE reducing sample buffer (0.5 M tris-HCl pH 6.8, 10% glycerol, 2% SDS, 0.1 mM 2-mercaptoethanol, 0.01% bromophenol blue), heated for 10 min at 95°C and electrophoresed on a 4-20% gradient SDS-PAGE. The gels were stained with Coomassie blue, dried, and then scanned with an Epson Expression 800 scanner using software v 1.01e. The dried gels were exposed to Kodak BioMax MS film with Kodak BioMax TranScreen HE at -80°C and the film developed with Kodak X-omat 200A processor. The autoradiography was scanned as above. With each gel a 21 step neutral density filter (Stouffer, IN, USA) was included to standardize optical density of proteins bands. The images were analyzed using ONE-DScan 2.05. The integrated OD of the autoradiograph was normalized by the integrated OD of the Coomassie blue-stained gel, to normalize the data for differences in protein loading. The other set of recombinant proteins was incubated as above but without radiochemical. The proteins were separated as above and the gel was stained with Pro-Q diamond to visualize proteins phosphorylated. The gel was fixed in 50% methanol 10% acetic acid, stained with Pro-Q diamond, destained with 20% ACN 50 mM sodium acetate pH 4, and scanned with Typhoon 9400 (excitation source 532 nm laser, emission filter 560 nm longpass). Then the gel was Coomassie blue stained to visualize total proteins and scanned as above. The Pro-Q diamond stain proteins were normalized to that of the Coomassie blue-

stained gel to normalize for protein loading. Recombinant PEVK protein expressed in *E. coli* was phosphorylated with 0.06 U/ $\mu$ l PKC $\alpha$  (Biomol) 2h at 30°C. The protein sample was then split with one half solubilized and the other had its PKC $\alpha$  inhibited with 37 nM bisindolylmaleimide I hydrochloride (Cell Signaling) and 0.7  $\mu$ M chelerythrine chloride (Sigma). The protein was then dephosphorylated by adding 1 U/ $\mu$ l PP1 (Calbiochem) 2h at 30°C. The solubilized proteins were separated by SDS-PAGE, 2-4% gradient gel, and transferred to PDVF membrane. The membranes were stained with Ponceau S for total protein and immunoblotted with phospho-specific polyclonal rabbit antibodies PS26 and PS170 (GenScript). Secondary antibody goat anti-rabbit conjugated with fluorescent dye with infrared excitation spectra was used for detection. The membranes were scanned (Odyssey Infrared Imaging System) and the images analyzed (See Online Fig. 5 for examples).

**Microarray studies.** We dissected the mice LV following TAC and collected them in *RNAlater*. The microarray experiments were performed as described previously<sup>6</sup>. Briefly, RNA was isolated using the Qiagen RNeasy Fibrous Tissue Mini Kit. RNA was amplified using the SenseAmp kit (Genisphere) and Superscript III reverse transcriptase enzyme (Invitrogen). Reverse transcription and dye coupling (Alexa Fluor 555 and Alexa Fluor 647 were used) was done using Invitrogen's superscript plus indirect cDNA labeling module. Half of each sample was incorporated with Alexa Fluor 555 and the other with Alexa Fluor 647. All the mouse titin (50 mer oligonucleotides) were spotted in triplicate on Corning Ultra GAPS glass slides. For each sample 750 ng of cDNA (Nanodrop, Thermo scientific) from each sample was hybridized (Ambion: Slide-Hyb buffer #1) for 16 h at 42 °C after which slides were scanned at 595 nm and 685 nm with an Array WoRx scanner. Spot finding was done with SoftWoRx Tracker and spot analysis with CARMA<sup>7</sup>. The analysis detects relative changes in the fluorescence of a probe (adult as compared to neonate). These changes are represented as a fold-difference and reflect the ratio of adult exon expression to neonate exon expression. A positive fold change indicates an increase in expression in adult relative to the neonate. A negative fold change indicates an increase in expression in neonate relative to the adult sample.

**Measurement of passive tension.** Small muscle strips (100-200  $\mu$ m in diameter, ~2mm in length) were dissected from the stored skinned papillary preparations. Passive tension

was measured with a strain gauge force transducer and fiber length was controlled by a high-speed motor. Preparations were attached to the motor arm and the force transducer via aluminum clips and lowered into a chamber containing relaxing solution. The width and the height of the fiber were measured and the cross-sectional area (CSA) was calculated assuming the cross section is elliptical in shape. The measured forces were then converted to tension (force/CSA). Typically three preparations were studied per heart and the average was obtained for each mouse. Sarcomere length (SL) was measured on line at 1 kHz by laser diffraction. At the beginning of each experiment, muscles were activated at SL 2.0  $\mu\text{m}$  (pCa 4.0) to measure residual active tension. Typically maximal activate tension was between  $\sim 30\text{-}40$  mN/mm<sup>2</sup>. For Online Table III, tensions are converted to stiffness; stiffness is defined as the slope of the linear fits between the SL ranges of 1.95-2.05  $\mu\text{m}$  as related to passive tension.

*Stretch-Hold Protocol:* Relaxed fibers were stretched (10%/sec) from their slack length (mouse  $\sim 1.85$   $\mu\text{m}$ ) to a SL of 2.15  $\mu\text{m}$ , followed by a 90 second hold. At the end of the “hold” the fiber was released back to slack length and allowed to rest 12 minutes before the next stretch. Muscles were stretched 4 times in order to show reproducibility of the force curve. Muscles were thoroughly rinsed in 20 mM BDM, a know inhibitor of actomyosin interaction that abolishes active isometric force development and stretches were repeated. For the *PP1-treatment Protocol* muscles were treated similar to the above protocol where a baseline force curve was determined prior to PP1-treatment. Following baseline determination muscles were treated in-chamber with PP1,  $\alpha$ -isoform, rabbit muscle, recombinant, expressed in E. coli (Calbiochem) (0.5 U/ $\mu\text{l}$ ) for 2 hours, stretching at every 20 minute interval. To determine titin and collagen contribution to passive force, thick and thin filaments were extracted from the sarcomere, removing titin’s anchors in the sarcomere<sup>8</sup>. The remaining force, assumed to be collagen based, was subtracted from the pre-extraction forces to determine titin-specific forces (for details, see<sup>8</sup>).

**Statistics.** Data are presented as mean  $\pm$  SEM. Group significance was defined using ANOVA followed by Tukey-Kramer multiple comparison test; SL significance was determined using 2-way ANOVA; Student’s *t*-test was used in Fig. 6A, inset; probability values  $<0.05$  were taken as significant and are indicated on figures as: HF and CHF significant from control, \* $P < 0.05$ ; CHF significant from HF, # $P < 0.05$  (two symbols:

$P < 0.01$  and 3 symbols:  $P < 0.001$ ). ANOVA with a linear model that incorporates terms to account for experimental variability was used in analysis of microarray data (for details see Greer et al., 2006). Linear regression analysis was used as necessary for correlations, \* $P < 0.05$ .

1. Li YH, Reddy AK, Taffet GE, Michael LH, Entman ML, Hartley CJ. Doppler evaluation of peripheral vascular adaptations to transverse aortic banding in mice. *Ultrasound Med Biol*. 2003;29:1281-9.
2. deAlmeida AC, van Oort RJ, Wehrens XH. Transverse aortic constriction in mice. *J Vis Exp*. 2010.
3. Liao Y, Ishikura F, Beppu S, Asakura M, Takashima S, Asanuma H, Sanada S, Kim J, Ogita H, Kuzuya T, Node K, Kitakaze M, Hori M. Echocardiographic assessment of LV hypertrophy and function in aortic-banded mice: necropsy validation. *Am J Physiol Heart Circ Physiol*. 2002;282:H1703-8.
4. Radke MH, Peng J, Wu Y, McNabb M, Nelson OL, Granzier H, Gotthardt M. Targeted deletion of titin N2B region leads to diastolic dysfunction and cardiac atrophy. *Proc Natl Acad Sci U S A*. 2007;104:3444-9.
5. Lahmers S, Wu Y, Call DR, Labeit S, Granzier H. Developmental control of titin isoform expression and passive stiffness in fetal and neonatal myocardium. *Circ Res*. 2004;94:505-13.
6. Buck D, Hudson BD, Ottenheijm CA, Labeit S, Granzier H. Differential splicing of the large sarcomeric protein nebulin during skeletal muscle development. *J Struct Biol*. 2010.
7. Greer KA, McReynolds MR, Brooks HL, Hoying JB. CARMA: A platform for analyzing microarray datasets that incorporate replicate measures. *BMC Bioinformatics*. 2006;7:149.
8. Wu Y, Cazorla O, Labeit D, Labeit S, Granzier H. Changes in titin and collagen underlie diastolic stiffness diversity of cardiac muscle. *J Mol Cell Cardiol*. 2000;32:2151-62.